# JCAMECH

# The effect of boundary conditions on the accuracy and stability of the numerical solution of fluid flows by Lattice-Boltzmann method

*Ali Bahrami, Ali Ghanvati, Azadeh Jafari\*and Mohammad Hassan Rahimian*

*School of Mechanical Engineering, College of Engineering, University of Tehran, Tehran, P.O.Box:11155-4563, Iran*

## ARTICLE INFO

## ABSTRACT

The aim of this study is to investigate the effect of boundary conditions on the accuracy and stability of the numerical solution of fluid flows in the context of single relaxation time Lattice Boltzmann method (SRT-LBM). The fluid flows are simulated using regularized, No-slip, Zou-He and Bounce Back boundary conditions for straight surfaces in a lid driven cavity and the two-dimensional flow in a channel. The solutions for all types of the boundary conditions show good agreement with numerical references and exact solutions. The cavity pressure contours at low relaxation time show drastic perturbations for Zou-He boundary condition, whereas, the perturbation is ignorable for regularized boundary condition. At High Reynolds number, severe velocity gradients are major reason for numerical instabilities. Therefore, regularized boundary condition, which considers the velocity gradient in its calculation, has better numerical stability comparing the Zou-He boundary condition. Overall, the selection of appropriate boundary condition depends on the flow regime and Geometry. The proper boundary conditions at low Reynolds numbers are Zou-He and Bounce Back boundary conditions, and at high Reynolds numbers, regularized and No-slip boundary conditions are recommended.

## 1. Introduction

Nowadays, computational fluid dynamics (CFD) help solve complex problems. Lattice Boltzmann method (LBM) is one of CFD methods, which are used on a mesoscopic scale. Instead of considering one particle of matter or an infinitesimal control volume, a group of particles is considered to derive the governing equations, based on the kinetic theory of gases[1, 2]. LBM is composed of two main processes: Collision between particles and streaming of particles[1, 2]. Here, the concept of particles is a fictitious particle which is obtained by probability distribution functions of the real particles[2]. LBM is widely used to simulate the flow in porous media, two or multi-phase flow, Newtonian and non-Newtonian fluids[3]. Obtaining probability distribution functions based on macroscopic quantities such that they satisfy conservation laws is an important issue in LBM. This issue reveals itself the most when applying boundary conditions on the Boltzmann equation. Various methods are proposed for boundary conditions. These methods include applying different boundary conditions, such as Dirichlet and Neumann, on straight and curved boundaries.

Different boundary conditions are used for fixed and moving boundaries. Boundary conditions can also be categorized to straight and curved boundaries, based on geometry. Bounce back boundary condition is the most common one[1]. The main idea behind this method, which is adapted from lattice gas cellular automata (LGCA) method[4], is to redistribute the fictitious particle in the opposite direction of the bulk flow direction on solid boundaries. Various researchers calculated probability distribution functions of curved boundaries using Bounce Back boundary and various interpolations and extrapolations Methods [5-10]. It's worth mentioning that the Bounce Back method is a simple, robust method and complies with conservation laws perfectly[7]. For straight boundaries, different approaches were used to expand the boundary conditions in which the relations obtained independently and from equation independent of macroscopic quantities. Bounce Back, Zou-He, No-slip and regularized boundary conditions are of the most important methods in applying macroscopic quantities to boundaries[11, 12]. Vershaeve proposed two non-slip boundary conditions for fixed boundaries. Considering that the diagonal elements of the strain matrix are zero for a straight boundary, he proposed new relations to calculate the non-equilibrium term of probability distribution function. This method can be used for relaxation frequencies up to 2 [12]. Latt et al. investigated the stability and the accuracy of second order regularized and Zou-He boundary conditions for different geometries. The results showed that selection of boundary condition depends on the flow regime

and geometry[11]. In addition, Vershaeve presented an algorithm to find unknown probability distribution functions on no slip curved boundaries by combining regularized and non-slip methods[13]. Malaspinas et al. presented a second-order boundary condition based on regularized method for straight boundaries which can be used for all computational nodes including flow corners[3]. Chopard and Dupuis proposed a boundary condition for fixed walls which converges more rapidly than the second order Bounce Back method[14]. Arun and Satheesh simulated a two-sided lid-driven cavity. They used Zou-He method for moving boundaries and Bounce Back method for fixed boundaries[15]. Hou and Zou performed an accuracy analysis on lid-driven cavity to evaluate the accuracy of LBM. The results of comparing their method with other numerical solutions indicate high accuracy of LBM in a wide range of Reynolds numbers. There were some perturbations found in cavity pressure contours in the upper corners of the cavity[16]. Izham et al. studied the high Reynolds numbers flow in a cavity and a 2D flow around a cylinder, using regularized lattice Boltzmann method (RLBM). There are some perturbations in cavity pressure contours[17]. Yu et al. removed instabilities through improving the mesh around the upper corners of the cavity, using the multi-block method[18]. Since boundary condition is one of the most important factors in perturbation development in solution field, using the best method of applying boundary conditions regarding the flow regime is of great importance. Due to the perturbations in cavity corners of studies using SRT-LBM model, it seems essential to investigate and compare the effect of different boundary conditions in stability and accuracy of solutions.

In this paper, we aim to study the effect of different boundary conditions on the straight wall in the context of LBM and compare the numerical results in lid-driven cavity and 2D channel flows. For each geometry, first we investigate the effect of full regularized and Zou-He boundary conditions for both moving and fix walls in terms of accuracy and convergence rates. Regarding the results of each section we combine the superior boundary condition, either Zou-He or regularized with other types, B No-slip, C No-slip and Bounce Back. In section 2, LBM governing equations are presented. In section 3, boundary conditions are introduced. In section 4, the numerical results of lid-driven cavity flow and flow inside a 2D channel are presented and finally, the conclusion of this paper is presented in section 5.

## 2. Lattice Boltzmann Method Using BGK Approximation

The Boltzmann equation in general form can be written as[2]:

$$\frac{\partial f}{\partial t} + \vec{c} \cdot \nabla_x f + \frac{\vec{F}}{m} \cdot \nabla_c f = \Omega(f) \tag{1}$$

Where $f$, is the probability distribution function, $\vec{c}$, is the velocity vector, $\vec{F}$, is the external force acting on the particle, $m$, is the particle mass, $\nabla_x$ is gradient respect to $x$ and $\nabla_c$ is gradient respect to the velocity and $\Omega(f)$ represents the Collision between particles. Using BGK model to approximate $\Omega(f)$ and ignoring external forces, the Boltzmann equation can be rewritten as below [1, 2, 12].

$$f(\vec{x} + \vec{c}\Delta t, t + \Delta t) - f(\vec{x}, t) = -\frac{\Delta t}{\tau}\left(f(\vec{x}, t) - f^{eq}(\vec{x}, t)\right) \tag{2}$$

where $\tau$ is the relaxation time and $f^{eq}$, is the probability distribution function of particles in the equilibrium. Eq. (2) includes two processes of particle collision and streaming. The discretized Boltzmann equation in limited directions is known as LBM which specified with common lattices like as D2Q9 and others[1]. Both collision and streaming in the LBM can be written as Eqs. (3-a) and (3-b) respectively that $f_i$ is the probability distribution function in the ith direction.

$$\tilde{f}_i(\vec{x}, t) - f_i(\vec{x}, t) = -\frac{1}{\tau}\left(f_i(\vec{x}, t) - f_i^{eq}(\vec{x}, t)\right) \tag{3-a}$$

$$f_i(\vec{x} + \vec{c}\Delta t, t + \Delta t) = \tilde{f}_i(\vec{x}, t) \tag{3-b}$$

The probability distribution function $f^{eq}$ can be calculated by Eq. (4). At first $f^{eq}$ is considered as the Maxwell's distribution function, which is an exponential function. Using the Taylor expansion and low Mach number (Ma) assumption, the Eq. (4) will be achieved and its truncation error is the order of $O(\text{Ma}^2)$ [2, 12, 19].

$$f_i^{eq} = t_i \rho(\vec{x}, t)\left[1 + \frac{\vec{c}_i \cdot \vec{u}}{c_s^2} + \frac{\boldsymbol{Q}_i : \vec{u}\vec{u}}{2c_s^4}\right] \tag{4}$$

where

$$\boldsymbol{Q}_i = \vec{c}_i \vec{c}_i - c_s^2 \boldsymbol{I} \tag{5}$$

D2Q9 lattice is one of the most popular lattices used in LBM. Coefficients of $t_i$, lattice velocity vectors, $\vec{c}_i$, and lattice speed of sound, $c_s$, are listed in Table 1 for D2Q9 model [1, 2]. The units in the LBM is not physical and for the length, time and mass is considered *lu*, *ts* and *mu*, respectively[1]. Catching the physical amounts need to map data in the lattice unit to physical one[20].

**Table 1**. Required coefficients for D2Q9 lattice

| Lattice type | Lattice vectors $\vec{c}_i$ | $t_i$ | $c_s^2$ |
|---|---|---|---|
| D2Q9 | (0, 0) | 4/9 | |
| | (±1, 0), (0, ±1) | 1/9 | 1/3 |
| | (±1, ±1) | 1/36 | |

The macroscopic quantities such as density, momentum, $\vec{j}$, and second order moment, $\boldsymbol{\Pi}$, are given in Eqs. (6) to (8) respectively, based on the probability distribution function[12]:

$$\rho = \sum_i f_i = \sum_i f_i^{eq} \tag{6}$$

$$\vec{j} = \rho\vec{u} = \sum_i \vec{c}_i f_i = \sum_i \vec{c}_i f_i^{eq} \tag{7}$$

$$\boldsymbol{\Pi} = \sum_i \vec{c}_i \vec{c}_i f_i \tag{8}$$

Boltzmann equation using BGK approximation can be written in macroscopic form using Chapman–Enskog analysis. In other words, lattice Boltzmann method is equivalent to Navier-Stokes equation. Based on Chapman–

Enskog analysis, $f_i$ in Boltzmann equation can be expanded around an equilibrium value as:[12, 19]

$$f_i = f_i^{(0)} + \varepsilon f_i^{(1)} + \varepsilon^2 f_i^{(2)} + \ldots \approx f_i^{(0)} + \varepsilon f_i^{(1)} + O(\varepsilon^2) \tag{9}$$

where $\varepsilon$ is a small value. $f_i^{(0)}$ is the probability distribution function at equilibrium. So, Eq. (9) can be rewritten as:

$$f_i = f_i^{eq} + f_i^{neq} \tag{10}$$

$f_i^{neq}$ is the non-equilibrium part of probability distribution function and is usually approximated by $\varepsilon f_i^{(1)}$. Thus, LBM is a second-order method $O(\varepsilon^2)$. That is, LBM is a numerical solution with $O(\delta x^2, \delta t^2, \text{Ma}^2)$ of error. $\delta x$ is the grid spacing, $\delta t$ is the time step and Ma is the Mach number[13].

Regarding mass and momentum conservation laws of particles while colliding and thanks to Eqs. (6) to (8), we can conclude that[12]:

$$\sum_i f_i^{neq} = 0 \tag{11}$$

$$\sum_i \vec{c}_i f_i^{neq} = \vec{0} \tag{12}$$

Based on Chapman–Enskog analysis, $f_i^{(1)}$, kinematic viscosity and strain tensor can be calculated as [12]:

$$f_i^{(1)} = -\frac{t_i}{c_s^2 \omega}[\boldsymbol{Q_i} : \rho \nabla \vec{u} - \vec{c}_i \nabla : \rho \vec{u}\vec{u}$$
$$+ \frac{1}{2c_s^2}(\vec{c}_i \cdot \nabla)(\boldsymbol{Q_i} : \rho \vec{u}\vec{u})] \tag{13}$$

$$v = c_s^2 \left( \frac{1}{\omega} - \frac{1}{2} \right) \tag{14}$$

$$\boldsymbol{\Pi}^{(1)} = \sum_i \vec{c}_i \vec{c}_i f_i^{(1)} = -\frac{2c_s^2}{\omega}\rho \boldsymbol{S} \tag{15}$$

where $\omega = 1/\tau$ is the collision frequency and $\boldsymbol{S} = (\nabla \vec{u} + \nabla \vec{u}^T)/2$ is the strain tensor.

In order to keep the incompressibility assumption in our numerical simulation the Mach number should be less than about 0.3. This means that the maximum velocity threshold for D2Q9 lattice should be about 0.18 [2].

$$\text{D2Q9}: c_s^2 = \frac{1}{3} \rightarrow u_{\max,\text{LBM}} \le 0.18 \tag{16}$$

Considering flow dimensionless numbers are equal in both physical and lattice scales, Reynolds number based on lattice parameters is defined as,[2]

$$\text{Re} = \frac{u_{\text{LBM}} N c_s^2}{(\tau - 0.5)} \tag{17}$$

Where $u_{\text{LBM}}$ is the characteristic speed and $N$ is the lattice size along the characteristic length. Also in LBM, pressure can be calculated as, [1, 19]
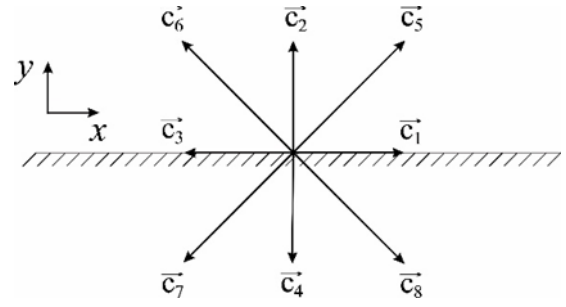
$$P = c_s^2 \rho \tag{18}$$



**Fig. 1.** Southern boundary node in a D2Q9 lattice

### 3. Boundary Conditions

Regarding the Streaming process of particles in LBM, fictitious particles are transferred to adjacent nodes. The fictitious particles in central nodes which move in various directions can move through and outside of the bulk flow. However, in the boundary nodes those directions of the lattice which doesn't receive information from outside of the bulk flow need boundary conditions to be determined. Moreover, transferring information from macroscopic to mesoscopic scale is a complicated task. In this study, four types of boundary conditions are evaluated: Bounce Back, B and C No-slip, Zou-He and regularized boundary conditions for straight and Dirichlet boundaries (Fig. 1).

### 3.1. Bounce Back Boundary Condition

This is the simplest boundary condition. When a particle collides with a fixed boundary, it will return in the opposite of the original direction. If boundary nodes are placed exactly on the solid boundary, a wet boundary is formed which is the simplest type of Bounce Back boundary condition. In other cases, the wall can be placed in between two rows of boundary nodes[1].

### 3.2. No-Slip Boundary Condition

The main idea of this type of boundary condition is based on the fact that the diagonal elements of the strain matrix are zero for a fixed boundary, which was applied to Eqs. (11), (12) and (15) by Vershaeve[12]. He provided a solvable system of equations of algebraic equations for $f_i^{neq}$. Through eliminating the equation containing the non-diagonal elements of the strain matrix. He was able to develop an indeterminate algebraic system of equations. Vershaeve proposed two kinds of boundary conditions (B and C), based on those $f_i^{neq}$ values that are aligned with the determined boundary ($i \in \{j \mid \vec{c}_j \cdot \vec{n} = 0\}$), $\vec{n}$ is the normal vector of boundary surface) to obtain a system of determinate algebraic equation. As a result, the system of equations close and unknown values of $f_i^{neq}$ are calculated [12, 21]

### 3.3. Zou-He Boundary Condition

In this method, the Bounce Back method was applied to $f_i^{neq}$ in line with the normal vector of the boundary. This can be seen, considering the symmetry in Eq. (13) [11]. It should be noted that influence of stress tensor is neglected in Zou-He method. Based on the idea of Zou-He, for the boundaries

shown in Fig. 1, Eqs. (6) and (7) are closed for four unknown variables: $\rho$, $f_2$, $f_5$ and $f_6$ [1, 22].

### 3.4. Regularized Boundary Condition

The method proposed by J.Latt known as the Regularized method, substitutes all values of probability distribution functions into the boundaries. He rewrote Eq. (13) using the symmetry of $\boldsymbol{Q}_i$ and $\boldsymbol{\Pi}_i^{(1)}$, and simplifying assumptions: [11, 19]

$$f_i^{(1)} \approx -\frac{\rho t_i}{c_s^2 \omega} \boldsymbol{Q}_i : \boldsymbol{S} = -\frac{t_i}{2c_s^4} \boldsymbol{Q}_i : \boldsymbol{\Pi}^{(1)} \qquad (19)$$

In Eq. (19), the value of $\boldsymbol{\Pi}^{(1)}$ is calculated using Eq. (15) and applying the Bounce Back method to $f_i^{neq}$ (similar to Zou-He method). The equations for the southern boundary while flow velocity is $(u,v)$, with corresponding to the Regularized method are presented in below. Employing the regularized and Zou-He boundary conditions for both velocity and pressure Dirichlet boundary conditions are similar.

$$f_i^{(1)} = \frac{t_i}{2c_s^4} \left( \boldsymbol{Q}_{ixx} \boldsymbol{\Pi}_{xx}^{(1)} + 2\boldsymbol{Q}_{ixy} \boldsymbol{\Pi}_{xy}^{(1)} + \boldsymbol{Q}_{iyy} \boldsymbol{\Pi}_{yy}^{(1)} \right)$$

$$\boldsymbol{\Pi}_{xx}^{(1)} = f_1 + f_3 + 2(f_7 + f_8) - \rho\left( -\frac{v}{3} + u^2 + c_s^2 \right)$$

$$\boldsymbol{\Pi}_{xy}^{(1)} = 2(f_7 + f_8) - \rho\left( -\frac{u}{3} + uv \right) \qquad (20)$$

$$\boldsymbol{\Pi}_{yy}^{(1)} = 2(f_4 + f_7 + f_8) - \rho\left( -v + v^2 + c_s^2 \right)$$

## 4. Results and Discussions

To evaluate the described boundary conditions, lid-driven cavity and flow through a channel are used. The evaluation criterion is based on the average relative error as:

$$\text{Average Relative Error} = \frac{1}{N} \sum_{j=1}^{N} \frac{\left| \vec{u}_j - \vec{u}_{j,\text{ref}} \right|}{\left| \vec{u}_{j,\text{ref}} \right|} \qquad (21)$$

The numerical results of lid-driven cavity are compared by the numerical results of reference [23] and for the 2D channel flow, the computed error is based on the exact solution. Also relative error approximation is used for convergence errors as below.

$$\text{Relative Convergence Error} = \left( \frac{\left| u_{i,j}^{k+1} - u_{i,j}^{k} \right|}{\left| u_{i,j}^{k} \right|}, \frac{\left| v_{i,j}^{k+1} - v_{i,j}^{k} \right|}{\left| v_{i,j}^{k} \right|} \right) \qquad (22)$$

### 4.1. Lid-driven Cavity

Lid-driven cavity is of significant importance in LBM due to the singular points on the upper corners. The intended geometry is the same as reference [23]. The geometry is shown in Fig. 2. The flow velocity is considered as unity and the kinematic viscosity is obtained as $1/\text{Re}$. The flow is solved for Reynolds numbers of 10, 100, 400 and 1000. In solving the flow using LBM, $\tau = 0.75$ for Reynolds numbers 10, 100 and 400, and $\tau = 0.6$ for Reynolds number 1000. Number of lattice nodes varies from 71 to 201 for Reynolds numbers 10 and 100, and from 121 to 261 for Reynolds number 400, and from 191 to 301 for Reynolds number 1000. Regarding the perturbations reported in pressure contours of Zou-He method for cavity geometry [16], $\tau = 0.75$ was chosen for Reynolds numbers of 10, 100 and 400 to ensure that there is no instability in the flow field. Number of lattice nodes are chosen in such a way that satisfies the conditions of Eq. (16). For Reynolds number 1000, the minimum number of lattice which satisfies the condition of Eq. (16) is equal to 464 at $\tau = 0.75$ which in regard has very high computational costs. So the $\tau = 0.6$ is chosen to reduce the computational cost due to maximum lattice nodes of 301. One of the main questions we would like to address in this section is to investigate the effect of Zou-He and Regularized boundary condition on bounding or minimizing the noise propagation in the corner of the cavity neighboring the moving wall. A cavity with fully regularized and full Zou-He boundary conditions are designed for this purpose, Table 2.
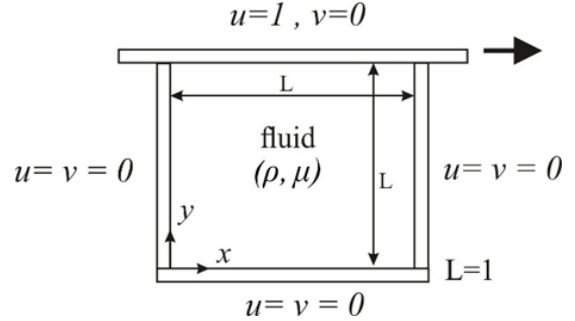


**Fig. 2.** schematic of Lid-driven cavity geometry

Figs. 3 & 4 show the average relative error for u and $v$ (velocity along $x$ and $y$ axes, respectively) versus the number of lattice points for Reynolds numbers 10, 100, 400 and 1000. Based on these figures, increasing lattice size leads to smaller errors as we expected. As it is obvious in these figures, the full regularized boundary condition has supremacy to the full Zou-He boundary condition with regards to average relative errors. Indeed, the regularized boundary condition takes into account the effect of the strain and velocity gradient specifically on moving boundary. So, it represents higher accuracy than the Zou-He method.

**Table 2**. Different boundary conditions used in lid-driven cavity

| State | Northern boundaries | Other Boundaries |
|-------|--------------------|------------------|
| 1 | Regularized | Regularized |
| 2 | Zou-He | Zou-He |
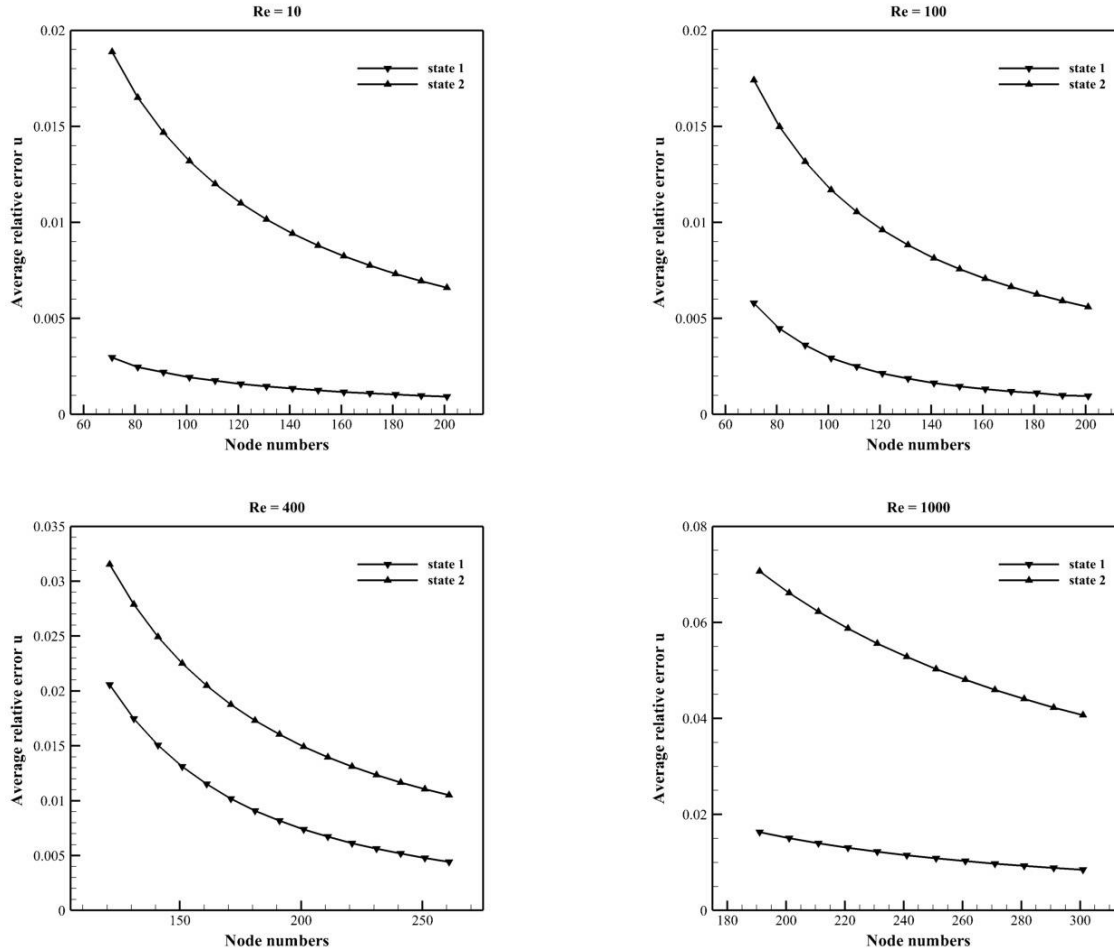


**Fig. 3.** Average relative error of *u* for Reynolds numbers 10,100,400 and 1000 in a lid driven cavity based on Table 2

Based on the latter results a natural question arises: how the accuracy of the numerical results will change if we combine the regularized boundary condition on moving wall (northern boundary) and couple this boundary with B No-slip and C No-slip types on fixed walls (like the arrangement of Table 3). The same numerical results are repeated for this case, fig 5 & 6. The accuracy of full regularized boundary condition, state 1, is better that state 3 and state 4 for both relative error of *u* and *v* in all ranges of Reynolds numbers. The only exception is the relative error of velocity field for *v* in moderate Reynolds number that shows better accuracy with the combination of regularized boundary condition for the moving wall and No-slip boundary condition for fixed walls. Just for curiosity and comparison, the results of full Zou-He boundary condition are added to these two sets of figures.

**Table 3**. Combination of Regularized boundary condition with other boundary conditions used in lid-driven cavity

| State | Northern boundaries | Other Boundaries |
|-------|--------------------|------------------|
| 1 | Regularized | Regularized |
| 3 | Regularized | B No-slip |
| 4 | Regularized | C No-slip |
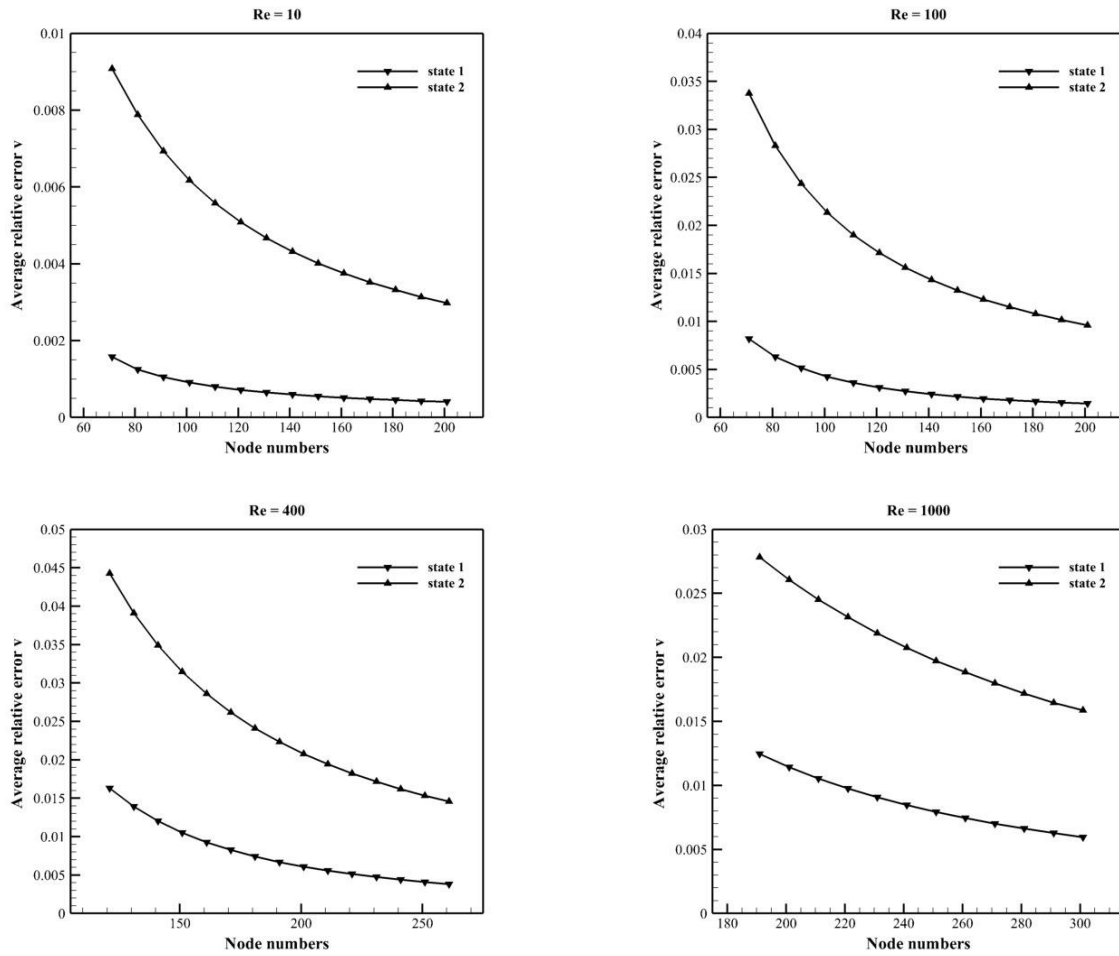
**Fig. 4.** Average relative error of $v$ for Reynolds numbers 10,100,400 and 1000 in a lid driven cavity based on Table 2

**Table 4**. Number of iterations required for convergence for Reynolds numbers of 100 and 400 and error of $10^{-8}$

| Re | Convergence error | State 1 | State 2 | State 3 | State 4 |
|----|-------------------|---------|---------|---------|---------|
| 100 | $10^{-8}$ | 29934 | 56641 | 26877 | 26558 |
| 400 | $10^{-8}$ | 137049 | 134392 | 45897 | 45892 |

Fig. 7 shows the cavity pressure contours for Reynolds number 100. These contours are plotted for a $101\times101$ lattice in two relaxation times; $\tau = 0.6$ and $\tau = 0.75$. The Bounce Back boundary condition is applied for all fixed boundaries and Zou-He and Regularized boundary conditions are applied on the moving boundary. According to the Fig. 7, numerical instability is observed in the upper corner of the cavity for $\tau = 0.6$ which is so widespread in Zou-He method but so small in regularized method. No instability is seen in $\tau = 0.75$ for regularized method but Zou-He method suffers from a small instability.

$u$ and $v$ diagrams aligned middle lines of $x = 1/2$ and $y = 1/2$ respectively for Reynolds numbers 1000 and 201

lattice nodes are shown in Fig. 8. To achieve better readability, just the state 1 of Table 2 is compared by the numerical results of reference [23] that has a great agreement with those solutions.

Another important factor in evaluation the boundary condition efficiency is the number of iterations required for convergence. For the lid-driven cavity, with the maximum relative convergence error of $10^{-8}$ (Eq. 22), the numbers of iterations required for convergence are listed in Table 4 for Reynolds numbers of 100 and 400.
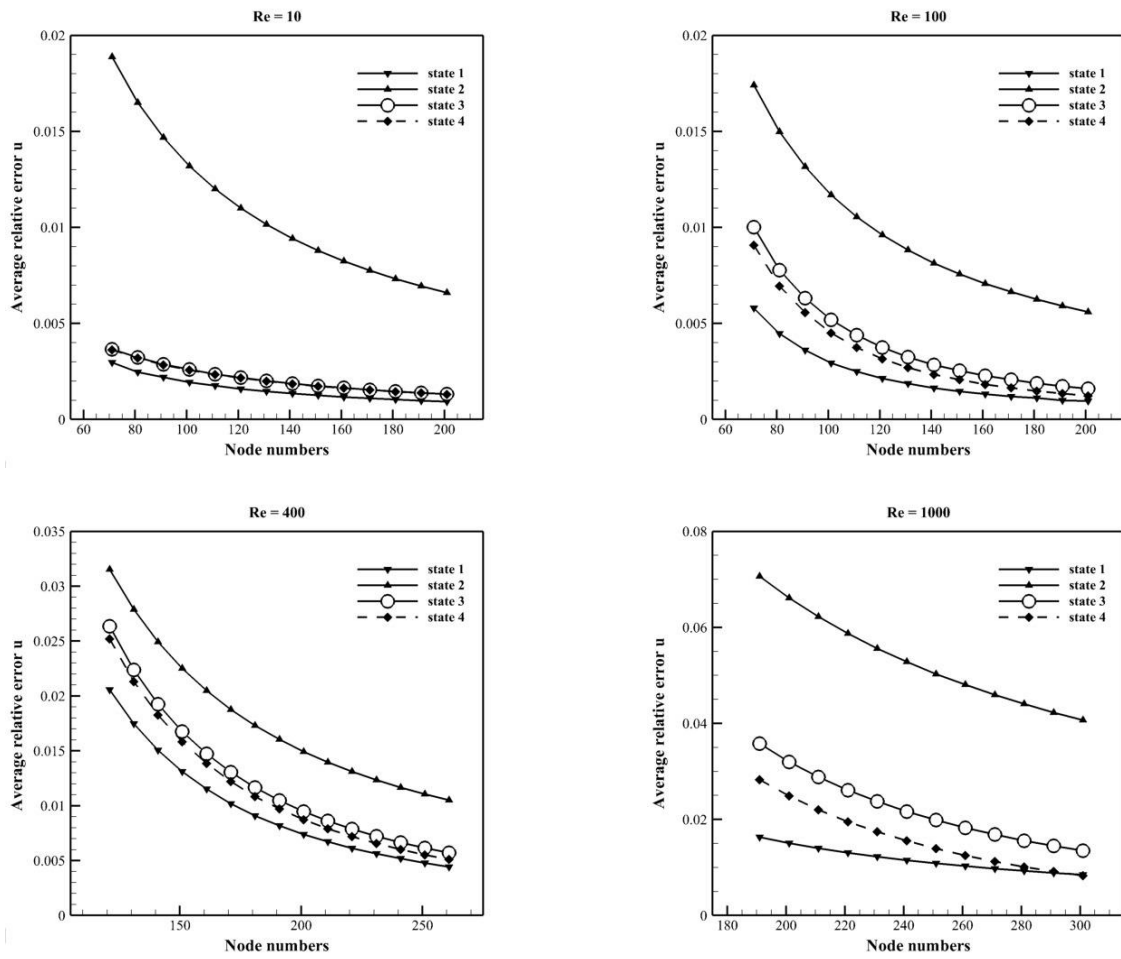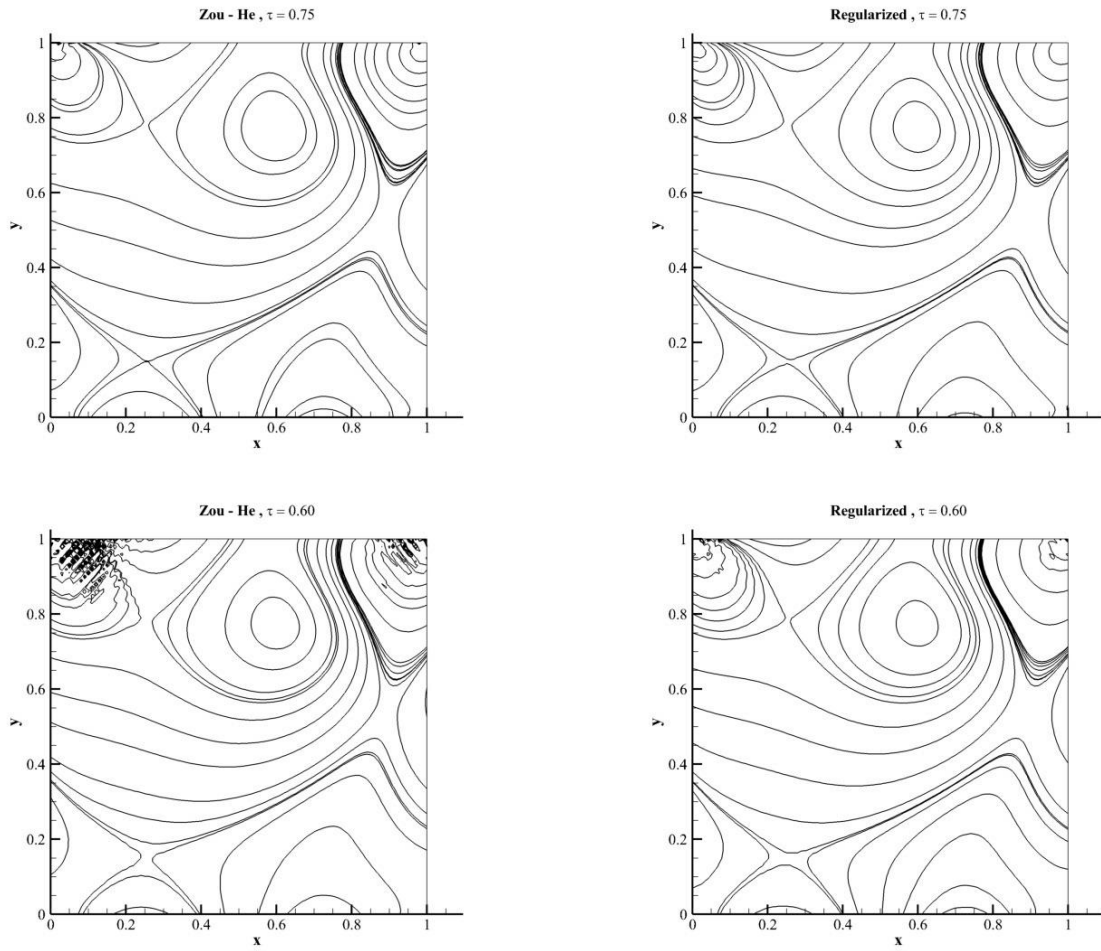
**Fig. 5.** Average relative error of $u$ for Reynolds numbers 10,100,400 and 1000 in a lid driven cavity based on Table 3
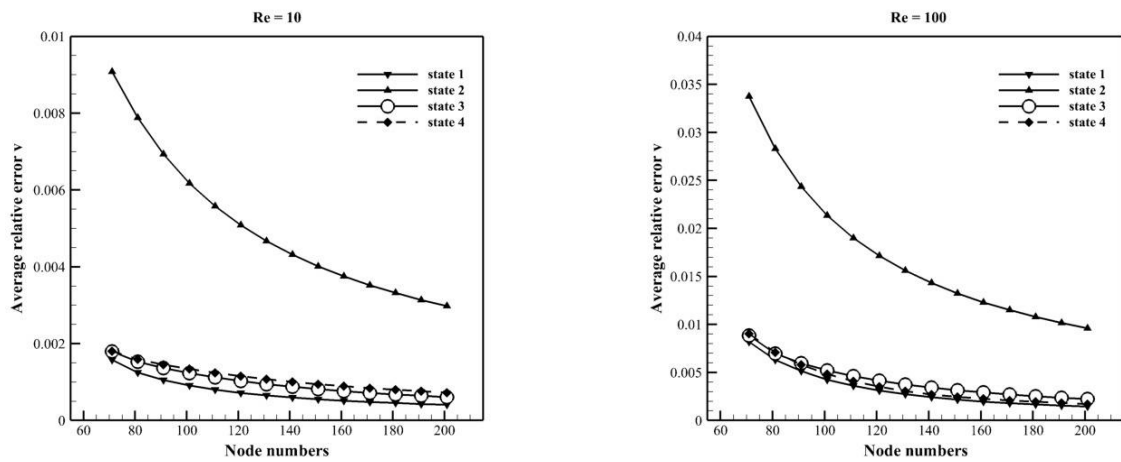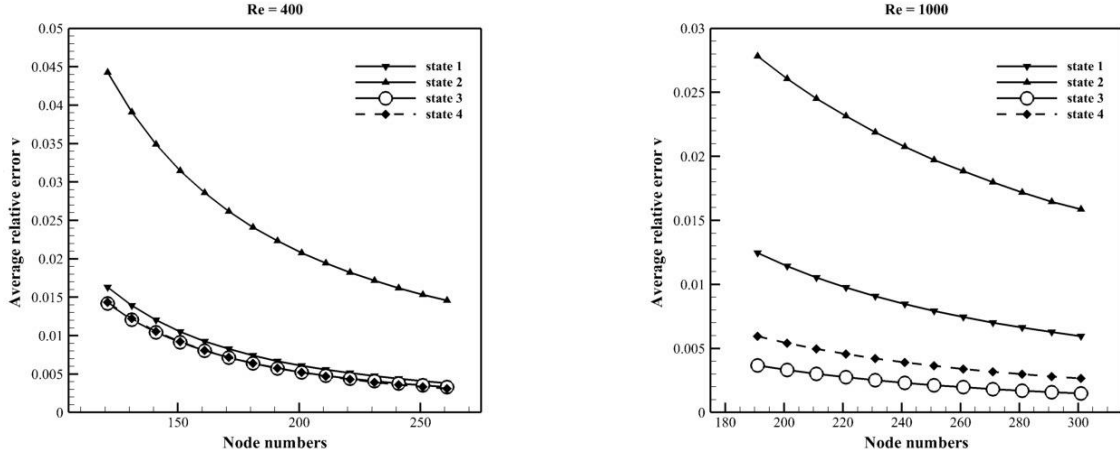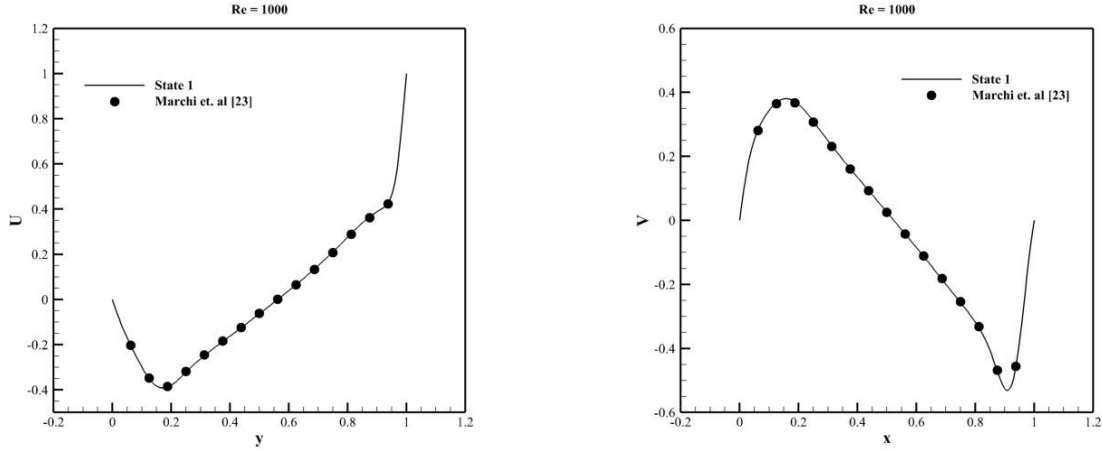
**Fig. 6.** Average relative error of $v$ for Reynolds numbers 10,100,400 and 1000 in a lid driven cavity based on Table 3



**Fig. 7.** Cavity pressure contours for Zou-He and regularized method applied to moving boundary for Reynolds number of 100 and in a 101×101 lattice (Bounce Back method was applied to other boundaries)

**Fig. 8.** $u$ and $v$ plots for middle lines of $x = 1/2$ and $y = 1/2$ respectively, and Reynolds number of 1000, in state 1 and for a $201 \times 201$ lattice

**Table 5**. Different boundary conditions used in 2D-channel flow

| State | Input/Output boundaries | Other Boundaries |
|-------|------------------------|------------------|
| 1 | Regularized | Regularized |
| 2 | Zou-He | Zou-He |

*4.2. 2D Channel*

The other geometry studied in this paper is the 2D Poiseuille flow or, in other words, the flow inside a channel. The overview of this geometry is shown in Fig. 9. Fully developed velocity profile at the inlet and constant outlet pressure Boundary condition are employed. The No-slip condition is applied on the walls.
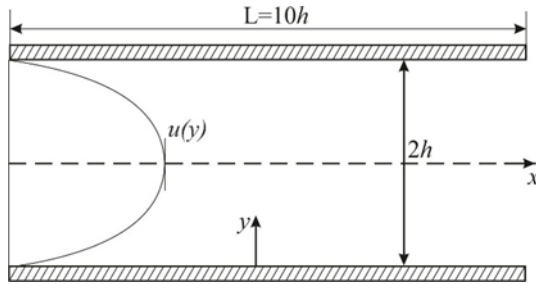


**Fig. 9:** 2D Poiseuille flow overview

The exact solution of the flow is [24]:

$$u_{\text{exact}}(y) = 6u_{\text{ave}} \frac{y}{2h}\left(1 - \frac{y}{2h}\right) \qquad (23)$$

where $u_{\text{ave}}$ is the average inlet velocity and the Reynolds number is defined based on this velocity as $Re = 2u_{\text{ave}}h/\nu$ in which $2h$ is the channel width and $\nu$ is the kinematic viscosity. The boundary conditions are listed below [24]:

$$y = 0, 2h \rightarrow u = 0$$

$$x = 0 \rightarrow u(y) = 6u_{\text{ave}} \frac{y}{2h}\left(1 - \frac{y}{2h}\right) \qquad (24)$$

$$x = L \rightarrow P = P_0 = \text{cte}$$

The outlet pressure is assumed as $P_0 = \alpha c_s^2$ in which $\alpha$ is the lattice to physical unit conversion factor. The flow is solved for Reynolds numbers of 10 and 100 and lattice nodes varying from 51 to 151 along the characteristic length using the discussed boundary conditions. Average relative errors versus lattice size is shown in Fig. 8. The same as the previous section, we are interested in examination full regularized and full Zou-He boundary conditions for a planar 2D flow (Table 5).

Fig. 10 demonstrates average velocity error for the streamwise velocity versus the number of lattice points. In contrast to the cavity, the full Zou-He boundary condition ends up to better accuracy than the full regularized boundary condition. Literally, the regularized boundary condition exhibits its advantage at high strain rate we counter in the cavity. In this simple shear flow at low Reynolds number, there is no dominance for regularized boundary condition.

Now the main question comes into being is the relation and combination of Zou-He boundary with other types of boundary conditions: B No-slip, C No-slip and Bounce Back (the arrangement are summarized in Table 6).
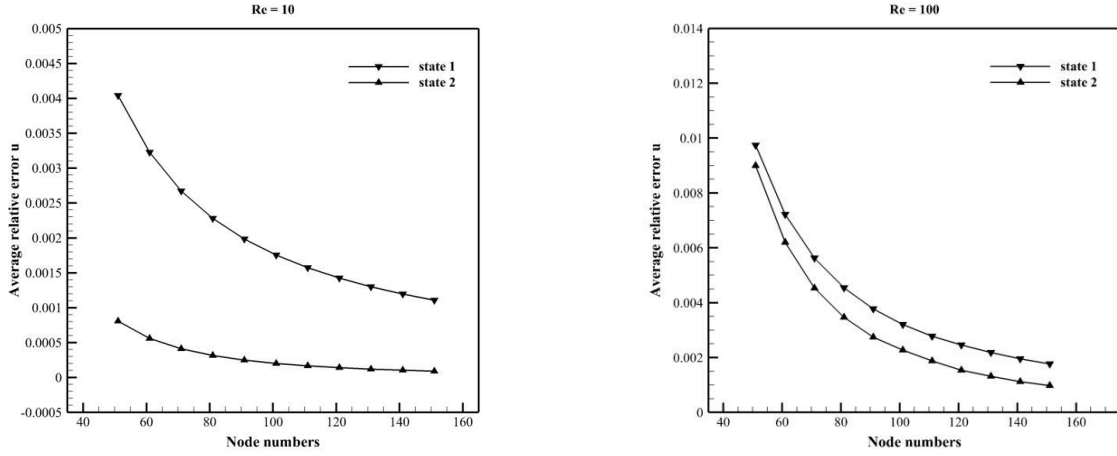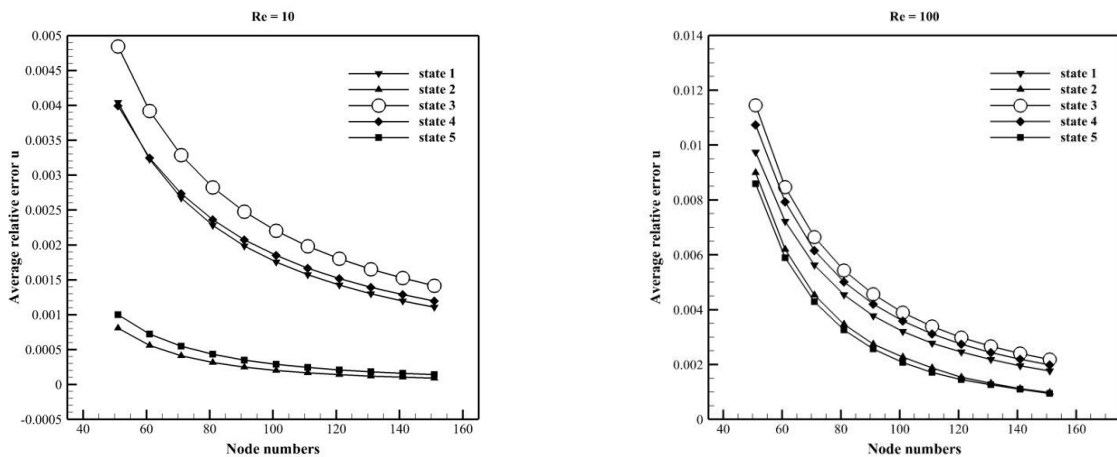
**Fig. 10.** Average relative error of *u* at *x* = L for Reynolds numbers of 10 and 100 in channel flow based on Table 5

**Table 6**. Different boundary conditions used in 2D-channel flow

| State | Input/Output boundaries | Other Boundaries |
|---|---|---|
| 2 | Zou-He | Zou-He |
| 3 | Zou-He | B No-slip |
| 4 | Zou-He | C No-slip |
| 5 | Zou-He | Bounce Back |

According to Fig. 11, increasing the computational nodes along the characteristic length will lead to more accurate solution. But as it can be seen in the figure, the disagreement of *states* 1, 3 and 4 with *states* 2 and 5 will decrease by increasing the Reynolds number. Since the effects of the strain and thus velocity gradients are not significantly important in low Reynolds numbers, and due to the fact that these effects are considered in Regularized and No-slip boundary conditions, their truncation error leads to more discrepancy with Zou-He and Bounce Back methods. By increasing the Reynolds number, velocity gradient effects become more important and therefore, the absence of gradient terms in Zou-He and Bounce Back methods lead to larger errors and the disagreement of *states* 2 and 5 with the other *states* will be minimized.



**Fig. 11.** Average relative error of *u* at *x* = L for Reynolds numbers of 10 and 100 in the channel flow based on Table 6
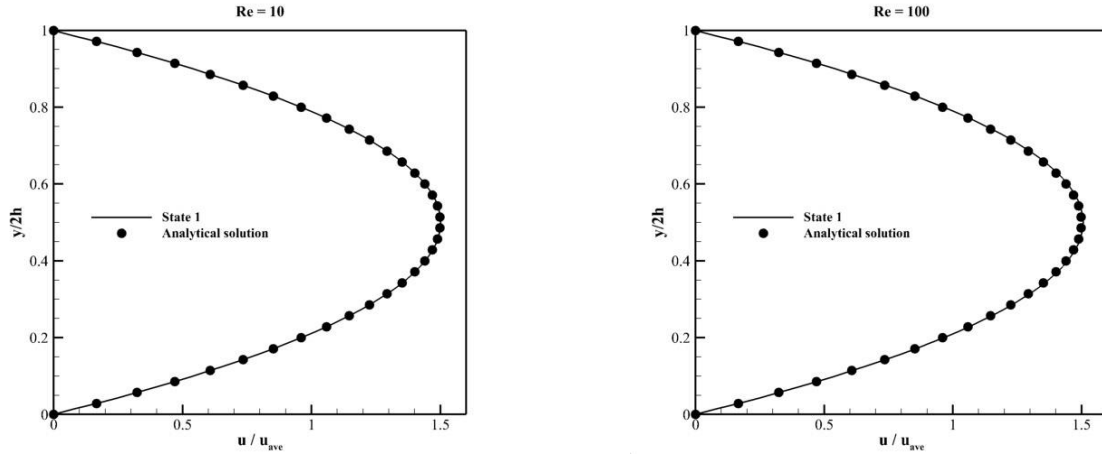
**Fig. 12.** $u/u_{ave}$ versus $y/2h$ in the outlet for a 71×351 lattice and Reynolds numbers of 10 and 100 and considering the state 1 for the boundaries conditions

**Table 7**. Number of iterations required for convergence for Reynolds numbers of 10 and 100 and error of $10^{-8}$

| Re | Convergence error | State 1 | State 2 | State 3 | State 4 | State 5 |
|---|---|---|---|---|---|---|
| 10 | $10^{-8}$ | 197813 | 201490 | 201558 | 201581 | 201494 |
| 100 | $10^{-8}$ | 120589 | 225511 | 226346 | 226857 | 225515 |

The streamwise velocity profile at the outlet for a 71×351 lattice and Reynolds numbers equal 10 and 100 with regularized boundary condition, state1, is shown in Fig. 9. According to this, the numerical solutions are in great agreement with the exact solution.

The numbers of iterations required for convergence based on Eq. (22) are listed in Table 7. It can be said that increasing Reynolds number enhances the convergence rate for regularized boundary condition. To evaluate the effects of boundary conditions applied to the inlet and outlet in comparison to the boundary conditions applied to the walls, the Regularized boundary condition was chosen for the inlet and outlet and B No-slip boundary condition was selected for the walls. The iterations were 197932 for Reynolds number of 10 and 121318 for Reynolds number of 100, which indicate the importance role of the inlet, and outlet boundary conditions play in the convergence.

Exceptionally, for state 1, the required iteration numbers decrease by increasing the Reynolds numbers. So, for this special test case, the convergence error versus the iteration number for three different Reynolds numbers, 10, 100 and 400 is plotted in Fig. 13. We review the number of iterations required for convergence in a 91×451 lattice for Reynolds numbers of 10, 100 and 400. Convergence errors against the required iterations number plots are shown in Fig. 13. By increasing the Reynolds number, the fluctuation amplitude around the response increases, as well as the convergence rate. Therefore, reduction of iteration numbers are natural. This happens due to the fact that there are velocity gradient terms in the Regularized boundary condition. When these terms are signified, the iteration numbers reduce. As can be seen in this figure, increasing the Reynolds number decreases the convergence rate and this origin from the velocity gradient

term in the Regularized boundary condition. At sufficiently high Reynolds number the velocity gradient in the flow becomes more important and regularized boundary condition shows its benefit at high Reynolds number.
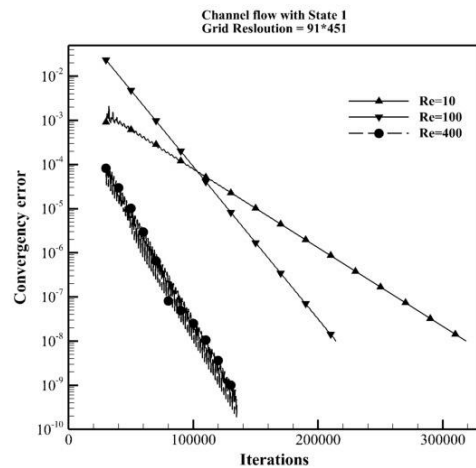


**Fig. 13.** Convergence error versus the iteration number for state 4 boundary conditions

## 5. Conclusions

In this paper, the flow in a lid-driven cavity and a 2D channel were studied using regularized, Zou-He, No-slip and Bounce Back boundary conditions. In all Figures, the relative error decreases by increasing the lattice size. Permanent existence of strong velocity gradients in the lid-driven cavity is the main factor of error. Thus, regularized and No-slip boundary conditions lead to a better accuracy compared to

Zou-He and Bounce Back methods. But for the 2D channel flow, $\partial u / \partial y$ is the only velocity gradient term, which is of little importance at low Reynolds numbers. As a result, it leads to higher truncation and round-off error in regularized and No-slip boundary conditions. Pressure contours inside the cavity were plotted in terms of $\tau$ and for regularized and Zou-He boundary conditions to evaluate the stability. According to these figures, strong velocity gradients lead to instability in the upper corners that regularized boundary condition resolves this problem. The numbers of iterations required for convergence were analyzed for both geometries. Results show that applying regularized and Zou-He methods on fixed boundaries will cause high computational costs. On the other hand, the influence of the inlet and outlet boundary condition on convergence rates in the channel flow was established clearly. Also, applying the regularized boundary lead to more rapid convergence rate in the channel flow.

Based on the discussions, in test cases where the velocity gradient is important, regularized method is much more efficient than Zou-He and much more stable. Thus, we can conclude that in high Reynolds number flows and in cases which perturbations can easily affect the fluid flow, the regularized method and in low Reynolds number flows, Zou-He method are more suitable. In the cases of strong velocity gradients on solid boundaries, regularized and No-slip methods are recommended while. at low velocity gradients, Zou-He and Bounce Back method are strongly adviced.

## Acknowledgment

## References

[1] M. C. Sukop, D. T. Thorne, 2010, *Lattice Boltzmann Modeling: An Introduction for Geoscientists and Engineers*, Springer Publishing Company, Incorporated,

[2] A. A. Mohamad, 2011, *Lattice Boltzmann method: fundamentals and engineering applications with computer codes*, Springer Science & Business Media,

[3] O. Malaspinas, B. Chopard, J. Latt, General regularized boundary condition for multi-speed lattice Boltzmann models, *Computers & Fluids,* Vol. 49, No. 1, pp. 29-35, 2011.

[4] D. A. Wolf-Gladrow, 2004, *Lattice-gas cellular automata and lattice Boltzmann models: an introduction*, Springer,

[5] M. h. Bouzidi, M. Firdaouss, P. Lallemand, Momentum transfer of a Boltzmann-lattice fluid with boundaries, *Physics of fluids,* Vol. 13, No. 11, pp. 3452-3459, 2001.

[6] Z. Guo, C. Zheng, B. Shi, An extrapolation method for boundary conditions in lattice Boltzmann method, *Physics of Fluids,* Vol. 14, pp. 2007-2010, 2002.

[7] I. Ginzburg, D. d'Humières, Multireflection boundary conditions for lattice Boltzmann models, *Physical Review E,* Vol. 68, 2003.

[8] H. Chen, C. Teixeira, K. Molvig, Realization of fluid boundary conditions via discrete Boltzmann dynamics, *International Journal of Modern Physics C,* Vol. 9, No. 08, pp. 1281-1292, 1998.

[9] X. Yin, J. Zhang, An improved bounce-back scheme for complex boundary conditions in lattice Boltzmann method, *Journal of Computational Physics,* Vol. 231, No. 11, pp. 4295-4303, 2012.

[10] T. Zhang, B. Shi, Z. Guo, Z. Chai, J. Lu, General bounce-back scheme for concentration boundary condition in the lattice-Boltzmann method, *Physical Review E,* Vol. 85, No. 1, 2012.

[11] J. Latt, B. Chopard, O. Malaspinas, M. Deville, A. Michler, Straight velocity boundaries in the lattice Boltzmann method, *Physical Review E,* Vol. 77, No. 5, 2008.

[12] J. C. G. Verschaeve, Analysis of the lattice Boltzmann Bhatnagar-Gross-Krook no-slip boundary condition: Ways to improve accuracy and stability, *Physical Review E,* Vol. 80, No. 3, 2009.

[13] J. C. Verschaeve, B. Müller, A curved no-slip boundary condition for the lattice Boltzmann method, *Journal of Computational Physics,* Vol. 229, No. 19, pp. 6781-6803, 2010.

[14] B. Chopard, A. Dupuis, A mass conserving boundary condition for lattice Boltzmann models, *International Journal of Modern Physics B,* Vol. 17, No. 01n02, pp. 103-107, 2003.

[15] S. Arun, A. Satheesh, Analysis of flow behaviour in a two sided lid driven cavity using lattice boltzmann technique, *Alexandria Engineering Journal,* Vol. 54, No. 4, pp. 795-806, 2015.

[16] S. Hou, Q. Zou, S. Chen, G. Doolen, A. C. Cogley, Simulation of cavity flow by the lattice Boltzmann method, *Journal of computational physics,* Vol. 118, No. 2, pp. 329-347, 1995.

[17] M. Izham, T. Fukui, K. Morinishi, Application of regularized lattice Boltzmann method for incompressible flow simulation at high Reynolds number and flow with curved boundary, *Journal of Fluid Science and Technology,* Vol. 6, No. 6, pp. 812-822, 2011.

[18] D. Yu, R. Mei, L.-S. Luo, W. Shyy, Viscous flow computations with the method of lattice Boltzmann equation, *Progress in Aerospace Sciences,* Vol. 39, No. 5, pp. 329-367, 2003.

[19] J. Latt, *Hydrodynamic limit of lattice Boltzmann equations*, Thesis, Universite De Geneve, 2007. English

[20] E. W. Llewellin, LBflow: An extensible lattice Boltzmann framework for the simulation of geophysical flows. Part I: theory and implementation, *Computers & Geosciences,* Vol. 36, No. 2, pp. 115-122, 2010.

[21] B. Müller, J. Verschaeve, *Boundary conditions for the lattice Boltzmann method: Mass conserving boundary conditions for moving walls*, Thesis, Institutt for energi og prosessteknikk, 2010.

[22] Q. Zou, X. He, On pressure and velocity boundary conditions for the lattice Boltzmann BGK model, *Physics of fluids,* Vol. 9, No. 6, pp. 1591-1598, 1997.

[23] C. H. Marchi, R. Suero, L. K. Araki, The lid-driven square cavity flow: numerical solution with a 1024 x 1024 grid, *Journal of the Brazilian Society of Mechanical Sciences and Engineering,* Vol. 31, pp. 186-198, 2009.

[24] F. M. White, 2015, *Fluid mechanics*, McGraw-Hill Higher Education, Fourth ed.